ELSEVIER

Physica A 240 (1997) 229–238

PHYSICA A

Viscometric effects in a dense hard-sphere fluid

José María Montanero[a], Andrés Santos[b,*]

[a] *Departamento de Electrónica e Ing. Electromecánica, Universidad de Extremadura, E-06071 Badajoz, Spain*

[b] *Departamento de Física, Universidad de Extremadura, E-06071 Badajoz, Spain*

Abstract

A recently proposed Monte Carlo simulation method for the Enskog equation is applied to uniform shear flow. This state is characterized by uniform density n and temperature T and a linear velocity profile: $\boldsymbol{u}(\boldsymbol{r}) = \mathbf{a}\cdot\boldsymbol{r}$, $a_{\alpha\beta} = a\delta_{\alpha x}\delta_{\beta y}$. In each unit time step Δt, the peculiar velocities $\{\boldsymbol{V}_i\}$ of N particles are updated in two stages. In the free streaming stage, the velocity $\boldsymbol{V}_i$ is changed into $\boldsymbol{V}_i \to \boldsymbol{V}_i - \mathbf{a}\cdot\boldsymbol{V}_i\,\Delta t$; in the collision stage, $\boldsymbol{V}_i \to \boldsymbol{V}_i - (\widehat{\boldsymbol{\sigma}}_i\cdot\boldsymbol{g}_{ij})\widehat{\boldsymbol{\sigma}}_i$ with probability equal to $4\pi\sigma^2\Theta(\widehat{\boldsymbol{\sigma}}_i\cdot\boldsymbol{g}_{ij})(\widehat{\boldsymbol{\sigma}}_i\cdot\boldsymbol{g}_{ij})\chi(n)n\,\Delta t$, where $\widehat{\boldsymbol{\sigma}}_i$ is a random unit vector, σ is the diameter of the spheres, $\boldsymbol{g}_{ij} \equiv \boldsymbol{V}_i - \boldsymbol{V}_j - \sigma\mathbf{a}\cdot\widehat{\boldsymbol{\sigma}}_i$, $\boldsymbol{V}_j$ being the velocity of a random partner j, and $\chi(n)$ is the equilibrium pair correlation function at contact. The kinetic and collisional transfer contributions to the pressure tensor are calculated as functions of density. The Navier–Stokes shear viscosity is seen to agree with the theoretical value. Furthermore, the nonlinear Burnett coefficients associated with normal stresses are obtained.

PACS: 05.60.+w; 47.50.+d; 83.20.Jp; 02.70.Lq
Keywords: Enskog equation; Monte Carlo simulation; Shear flow; Viscometric coefficients

1. Introduction

The simplest system to analyze non-equilibrium properties is a low-density gas of particles interacting via a short-range potential. In that case, the relevant local average quantities (such as the densities of conserved quantities and their fluxes) can be expressed as velocity integrals of the one-particle distribution function $f(\boldsymbol{r},\boldsymbol{v},t)$, whose time evolution is governed by the Boltzmann equation (BE) [1–3]. The assumptions implicit in the BE, in particular the hypothesis of molecular chaos or *stosszahlansatz*, are physically justified in the low-density limit [3]. On the other hand, as the density increases, structural effects become important, potential contributions to the fluxes dominate, and the BE is no longer adequate.

* Fax: +34 24 275428; e-mail: andres@unex.es.

PII S0378-4371(97)00146-5

With great physical insight, Enskog proposed in 1922 [4] a semi-phenomenological equation based on the BE for hard spheres of diameter σ. Two important changes in the Boltzmann collision integral were introduced: (a) the centers of two colliding particles are separated by a distance equal to σ; (b) the collision frequency is multiplied by a factor χ that takes into account the spatial correlations between a pair of colliding particles. In the standard Enskog theory (SET) [1,2], χ is evaluated from the density at the midpoint, while in the revised Enskog theory (RET) [5], χ is given as a functional of the density field. The RET follows exactly from the BBGKY hierarchy in the limit of short-times starting from an uncorrelated initial state. This short-time limit does not entail any limitations on the density or space scale, so that the RET can be applied at high densities and at short wavelengths. Moreover, it admits both fluid and crystal equilibrium states as stationary solutions [6].

In spite of the potential of the RET for describing fluid, crystal, and metastable states near and far from equilibrium, its mathematical intricacy has hindered practical applications. Two alternatives have been recently proposed to cope with this problem. First, a simulation Monte Carlo method has been introduced to solve numerically the RET [7]; second, a simple kinetic model has been constructed that retains the main features of the RET [8]. In this paper we will be concerned with the first approach.

The simulation method proposed in Ref. [7] is a natural adaptation to the Enskog equation of the direct simulation Monte Carlo (DSMC) method to solve the BE [9,10]. A previous algorithm (CBA) [11] is consistent with the equilibrium equation of state for hard spheres but provides transport coefficients different from those of the Enskog equation. In Ref. [7] the simulation was applied to the uniform shear flow (USF) state at a rather large density $n\sigma^3 = 0.8$ and was shown to be consistent with the Enskog equation for the pressure tensor at local equilibrium, the viscous heating equation, and the Navier–Stokes shear viscosity η. The objective here is to extend that analysis by comparing the density dependence of η, as obtained from the simulations, with the theoretical function obtained from the Enskog equation. As an illustration of non-Newtonian effects obtained from the simulations, we show the density dependence of viscometric coefficients associated with normal stresses to Burnett order. The simulation values of these coefficients present a good agreement with the theoretical expressions recently derived from the Enskog equation [12]. In addition, the super-Burnett coefficient of the non-Newtonian shear viscosity is considered.

The paper is organized as follows. The Enskog equation and the USF state are briefly summarized in Section 2. The simulation Monte Carlo method, especialized to the USF, is described in Section 3. Finally, the results are presented and discussed in Section 4.

2. The Enskog equation for a fluid under uniform shear flow

The Enskog equation reads [1–3]

$$\left(\frac{\partial}{\partial t}+\boldsymbol{v}\cdot\frac{\partial}{\partial \boldsymbol{r}}\right)f(\boldsymbol{r},\boldsymbol{v},t)=\sigma^2\int d\boldsymbol{v}_1\int d\widehat{\boldsymbol{\sigma}}\,\Theta(\widehat{\boldsymbol{\sigma}}\cdot\boldsymbol{g})(\widehat{\boldsymbol{\sigma}}\cdot\boldsymbol{g})$$
$$\times[\chi(\boldsymbol{r},\boldsymbol{r}-\boldsymbol{\sigma})f(\boldsymbol{r},\boldsymbol{v}',t)f(\boldsymbol{r}-\boldsymbol{\sigma},\boldsymbol{v}_1',t)$$
$$-\chi(\boldsymbol{r},\boldsymbol{r}+\boldsymbol{\sigma})f(\boldsymbol{r},\boldsymbol{v},t)f(\boldsymbol{r}+\boldsymbol{\sigma},\boldsymbol{v}_1,t)]\,. \tag{1}$$

Here $\Theta(x)$ is the Heaviside function, $\boldsymbol{g}\equiv\boldsymbol{v}-\boldsymbol{v}_1$, $\boldsymbol{\sigma}=\sigma\widehat{\boldsymbol{\sigma}}$, $\boldsymbol{v}'=\boldsymbol{v}-(\widehat{\boldsymbol{\sigma}}\cdot\boldsymbol{g})\widehat{\boldsymbol{\sigma}}$, and $\boldsymbol{v}_1'=\boldsymbol{v}_1+(\widehat{\boldsymbol{\sigma}}\cdot\boldsymbol{g})\widehat{\boldsymbol{\sigma}}$. In the RET, χ is the (local) equilibrium pair correlation function at contact in a *non-uniform* state. That means that χ is a functional of the number density field

$$n(\boldsymbol{r},t)=\int d\boldsymbol{v}\,f(\boldsymbol{r},\boldsymbol{v},t)\,. \tag{2}$$

In a similar way, the momentum density, $mn(\boldsymbol{r},t)\boldsymbol{u}(\boldsymbol{r},t)$, and the internal energy density, $\frac{3}{2}n(\boldsymbol{r},t)k_BT(\boldsymbol{r},t)$, can be obtained as velocity moments of f. Here, m is the mass of a particle, $\boldsymbol{u}(\boldsymbol{r},t)$ is the local flow velocity, k_B is the Boltzmann constant, and $T(\boldsymbol{r},t)$ is the local temperature. The Enskog equation, Eq. (1), leads to conservation equations for the densities of mass, momentum, and energy, from which one can identify the fluxes of momentum (pressure tensor) and internal energy (heat flux). Both have kinetic as well as collisional transfer contributions. For instance, the kinetic part, $\mathbf{P}^k$, of the pressure tensor $\mathbf{P}$ is

$$\mathbf{P}^k=m\int d\boldsymbol{v}\,\boldsymbol{V}\boldsymbol{V}f\,, \tag{3}$$

where $\boldsymbol{V}=\boldsymbol{v}-\boldsymbol{u}$ is the "peculiar" velocity, i.e. the velocity in the (local) Lagrangian frame. The expression for the collisional transfer contribution, $\mathbf{P}^c$, will be given below. Henceforth, the superscripts k and c will denote kinetic and collisional parts, respectively.

The Navier–Stokes constitutive equations are obtained from the standard Chapman–Enskog method [1,2]. In particular, the shear viscosity is

$$\eta=\frac{1}{\chi}(1+\tfrac{4}{15}\pi n\sigma^3\chi)^2\eta^0+\tfrac{4}{15}n^2\sigma^4\chi(\pi mk_BT)^{1/2}\,, \tag{4}$$

where η^0 is the shear viscosity for hard spheres given by the BE. Its value is [1]

$$\eta^0=\frac{5b}{16}\left(\frac{mk_BT}{\pi}\right)^{1/2}\sigma^{-2}\,, \tag{5}$$

with $b\simeq 1.0160$. One can also identify a kinetic contribution to the shear viscosity. Its expression is

$$\eta^k=\frac{1}{\chi}\,(1+\tfrac{4}{15}\pi n\sigma^3\chi)\,\eta^0\,. \tag{6}$$

Now we consider the USF state. It is characterized by a constant density ($n=\text{const}$), a uniform temperature ($\nabla T=0$), and a linear velocity field: $\boldsymbol{u}(\boldsymbol{r})=\mathbf{a}\cdot\boldsymbol{r}$, where $\mathbf{a}$ is a tensor with elements $a_{\alpha\beta}=a\delta_{x\alpha}\delta_{y\beta}$, a being the constant shear rate. This state

can be maintained at the expense of a monotonic increase of temperature (viscous heating) [13]:

$$\frac{3}{2} n k_B \frac{dT}{dt} = -aP_{xy} . \tag{7}$$

In molecular dynamics simulations it is usual to add a thermostat force to compensate for this heating effect and achieve a steady state [14]. Here, however, we do not introduce any thermostat. As a consequence, the mean free time τ monotonically decreases and so does the *reduced* shear rate $a^* = a\tau$. Thus, the state of the system becomes in time closer and closer to that of local equilibrium. Here we choose to define the mean free time as $\tau = \eta^0/\chi n k_B T$. The relationship between τ and the conventional Boltzmann time t_B is $\tau = \frac{5b}{4}\chi^{-1} t_B$.

At a microscopic level, the USF is characterized by a distribution function that becomes *uniform* when the velocities are expressed in the Lagrangian frame, i.e. $f(\boldsymbol{r}, \boldsymbol{v}, t) = \bar{f}(\boldsymbol{V}, t)$ with $\boldsymbol{V} = \boldsymbol{v} - \mathbf{a}\cdot\boldsymbol{r}$. In that case, the Enskog equation, Eq. (1), can be written as

$$\left(\frac{\partial}{\partial t} - \frac{\partial}{\partial \boldsymbol{V}}\cdot\mathbf{a}\cdot\boldsymbol{V}\right)\bar{f}(\boldsymbol{V},t) = \sigma^2\chi \int d\boldsymbol{V}_1 \int d\widehat{\boldsymbol{\sigma}}\,\Theta(\widehat{\boldsymbol{\sigma}}\cdot\boldsymbol{g})(\widehat{\boldsymbol{\sigma}}\cdot\boldsymbol{g}) \times [\bar{f}(\boldsymbol{V}',t)\bar{f}(\boldsymbol{V}_1',t) - \bar{f}(\boldsymbol{V},t)\bar{f}(\boldsymbol{V}_1,t)] , \tag{8}$$

where now $\boldsymbol{g} = \boldsymbol{V} - \boldsymbol{V}_1 - \mathbf{a}\cdot\boldsymbol{\sigma}$, $\boldsymbol{V}' = \boldsymbol{V} - (\widehat{\boldsymbol{\sigma}}\cdot\boldsymbol{g})\widehat{\boldsymbol{\sigma}}$, and $\boldsymbol{V}_1' = \boldsymbol{V}_1 + 2\mathbf{a}\cdot\boldsymbol{\sigma} + (\widehat{\boldsymbol{\sigma}}\cdot\boldsymbol{g})\widehat{\boldsymbol{\sigma}}$. Since in the USF the number density is a constant, there is no distinction between the SET and the RET. In both cases χ is uniform and its dependence on n arises from the equation of state of the fluid, i.e.

$$p_0 = n k_B T(1 + \tfrac{2}{3}\pi n^* \chi) , \tag{9}$$

where p_0 is the equilibrium hydrostatic pressure of a hard-sphere fluid and $n^* \equiv n\sigma^3$. Here we will use the Carnahan–Starling (CS) equation of state [15]:

$$\chi(n^*) = \frac{1 - (\pi/12)n^*}{(1 - (\pi/6)n^*)^3} . \tag{10}$$

In the particular case of USF, the general expression for the collisional transfer pressure tensor [7,8] becomes

$$\mathbf{P}^c(t) = \frac{m}{2}\sigma^3\chi \int d\boldsymbol{V} \int d\boldsymbol{V}_1 \int d\widehat{\boldsymbol{\sigma}}\,\widehat{\boldsymbol{\sigma}}\widehat{\boldsymbol{\sigma}}\Theta(\widehat{\boldsymbol{\sigma}}\cdot\boldsymbol{g})(\widehat{\boldsymbol{\sigma}}\cdot\boldsymbol{g})^2 \bar{f}(\boldsymbol{V},t)\bar{f}(\boldsymbol{V}_1,t) . \tag{11}$$

Eq. (8) admits solutions for arbitrary values of the shear rate and arbitrary initial conditions. From a physical point of view, it is expected that for sufficiently long times the distribution function adopts a form that is independent of the details of the initial conditions ("normal solution"). More explicitly, $\bar{f}(\boldsymbol{V},t) \to f^*(\boldsymbol{V}^*, a^*)$, where $\boldsymbol{V}^* = (2k_BT/m)^{-1/2}\boldsymbol{V}$ and $f^* = n^{-1}(2k_BT/m)^{3/2}\bar{f}$. Consequently, the reduced pressure tensor $\mathbf{P}/nk_BT$ associated with the normal solution is, at a given value of $n^*\chi$, a function of the reduced shear rate a^*.

In this paper we will be mainly interested in the transport properties for small (reduced) shear rates. In particular, the Navier–Stokes shear viscosity can be identified in the USF state as

$$\chi\frac{\eta}{\eta^0}=\lim_{a^*\to 0}\frac{-P_{xy}}{nk_BTa^*}\,. \tag{12}$$

Effects associated with normal stresses are characterized by the viscometric coefficients

$$\Psi_1=\lim_{a^*\to 0}\frac{P_{yy}-P_{xx}}{nk_BTa^{*2}}\,, \tag{13}$$

$$\Psi_2=\lim_{a^*\to 0}\frac{P_{zz}-P_{yy}}{nk_BTa^{*2}}\,. \tag{14}$$

These are non-linear Burnett coefficients (which are functions of the density parameter $n^*\chi$). Following the notation in Chapman and Cowling's monograph [1], they are given by $\Psi_1=-\varpi_2$, $\Psi_2=\varpi_2-\frac{1}{4}\varpi_6$ in the case of the Boltzmann equation; for hard spheres the corresponding numerical values are $\Psi_1\simeq -2.028$, $\Psi_2\simeq 0.172$. There is another non-linear Burnett coefficient related to normal effects, but that vanishes in the low-density limit. It measures the increase of the non-equilibrium "hydrostatic pressure" $p=\frac{1}{3}\mathrm{tr}\,\mathbf{P}$ with respect to its equilibrium value p_0, a phenomenon usually referred to as "shear dilatancy" [16]. To characterize this effect we define the coefficient

$$\gamma=\lim_{a^*\to 0}\frac{p-p_0}{nk_BTa^{*2}}\,. \tag{15}$$

These coefficients, along with their kinetic and collisional counterparts, have been recently derived as functions of density by Lutsko [12] from a perturbative solution of the Enskog equation to second order in the shear rate and to fourth order in velocity moments. It is found that $\Psi_1^k(n^*\chi)$ and $\gamma(n^*\chi)/(n^*\chi)^2$ are linear functions of $n^*\chi$, $\Psi_1(n^*\chi)=\Psi_1^{k2}(n^*\chi)/\Psi_1(0)$, $\Psi_2^k(n^*\chi)$ is a quadratic function, and $\Psi_2(n^*\chi)$ is a cubic function. Since a certain truncation is involved, the numerical coefficients in those functions are not exact, although they are good estimates. For instance, the coefficient b in the Boltzmann shear viscosity, Eq. (5), is $b=\frac{205}{202}\simeq 1.0149$, and $\Psi_1(0)=-\frac{85\,058}{42\,025}\simeq -2.024$, $\Psi_2(0)=\frac{3449}{20\,705}\simeq 0.167$.

Non-Newtonian effects in the shear viscosity appear to super-Burnett order. To characterize them, we introduce the coefficient

$$\eta_2=\lim_{a^*\to 0}\frac{-P_{xy}-\eta a}{nk_BTa^{*3}}\,. \tag{16}$$

To the best of our knowledge, this coefficient has not been determined before from the Enskog equation, even at zero density. According to a kinetic model of the RET [8], $\eta_2(n^*\chi)$ is a quartic function that takes negative values for small densities and becomes positive for large densities.

3. Enskog simulation Monte Carlo method

Recently, we have proposed a numerical algorithm, the Enskog simulation Monte Carlo (ESMC) method, to solve the Enskog equation, Eq. (1). The method is an extension of the celebrated DSMC method [9] to solve the Boltzmann equation. In fact, it reduces to Nanbu's version [10] in the low-density limit, i.e. when $\sigma(2k_BT/m)^{-1/2}\tau^{-1} \to 0$, $\chi \to 1$. For a detailed description of the ESMC method we refer the reader to Ref. [7]. Here we briefly describe its adaptation to deal with Eq. (8).

Let N be the number of particles. Since there is no space dependence in Eq. (8), only the velocities $\{\boldsymbol{V}_i,\ i=1,\ldots,N\}$ are stored at times $t=\Delta t, 2\Delta t, 3\Delta t,\ldots$, where $\Delta t \ll \tau$. At each time step, the velocities are updated in two stages: $\boldsymbol{V}_i(t) \xrightarrow{1} \widetilde{\boldsymbol{V}}_i(t) \xrightarrow{2} \boldsymbol{V}_i'(t)=\boldsymbol{V}_i(t+\Delta t)$. The first stage represents free streaming and is related to the second term on the left-hand side of Eq. (8). Such a term can be viewed as a non-conservative external force of the form $\boldsymbol{F}=-m\mathbf{a}\cdot\boldsymbol{V}$. Thus, in the free streaming stage

$$\widetilde{\boldsymbol{V}}_i=\boldsymbol{V}_i-\mathbf{a}\cdot\boldsymbol{V}_i\Delta t\,. \tag{17}$$

In the collision stage, the following steps are carried out for every particle $i=1,\ldots,N$. A random direction $\widehat{\boldsymbol{\sigma}}_i$ and a random partner particle $j\neq i$ are chosen with equiprobability. The important quantity is the dot product $(\widehat{\boldsymbol{\sigma}}_i\cdot\boldsymbol{g}_{ij})$, where $\boldsymbol{g}_{ij}\equiv\widetilde{\boldsymbol{V}}_i-\widetilde{\boldsymbol{V}}_j-\sigma\mathbf{a}\cdot\widehat{\boldsymbol{\sigma}}_i$. The collision with particle j is accepted with a probability equal to the collision rate times the time-step, namely $4\pi\sigma^2\chi n\Theta(\widehat{\boldsymbol{\sigma}}_i\cdot\boldsymbol{g}_{ij})(\widehat{\boldsymbol{\sigma}}_i\cdot\boldsymbol{g}_{ij})\,\Delta t$. If the collision is rejected, then $\boldsymbol{V}_i'=\widetilde{\boldsymbol{V}}_i$. Otherwise,

$$\boldsymbol{V}_i'=\widetilde{\boldsymbol{V}}_i-(\widehat{\boldsymbol{\sigma}}_i\cdot\boldsymbol{g}_{ij})\widehat{\boldsymbol{\sigma}}_i\,. \tag{18}$$

After the collision stage has finished for all the particles, the kinetic and collisional transfer contributions of the pressure tensor are evaluated as

$$\mathbf{P}^k=\frac{mn}{N}\sum_i\boldsymbol{V}_i'\boldsymbol{V}_i'\,, \tag{19}$$

$$\mathbf{P}^c=\frac{mn\sigma}{2\Delta tN}\sum_i(\widetilde{\boldsymbol{V}}_i-\boldsymbol{V}_i')\widehat{\boldsymbol{\sigma}}_i\,. \tag{20}$$

To improve the statistics, the results are averaged over a number $\mathcal{N}$ of independent replicas. The results presented in this paper have been obtained with $\mathcal{N}=10$, $N=10^5$, and $\Delta t=10^{-2}\tau$. Notice that Δt is not a constant but decreases in time.

4. Results and discussion

By applying the method outlined in the preceding section, we have followed the time evolution of the pressure tensor for values of $n^*\chi$ in the range $0.05\leqslant n^*\chi\leqslant 4.5$. According to the CS equation of state, Eq. (10), this corresponds to densities in the range $0.047\leqslant n^*\leqslant 0.891$. Although the RET is not expected to be accurate for densities

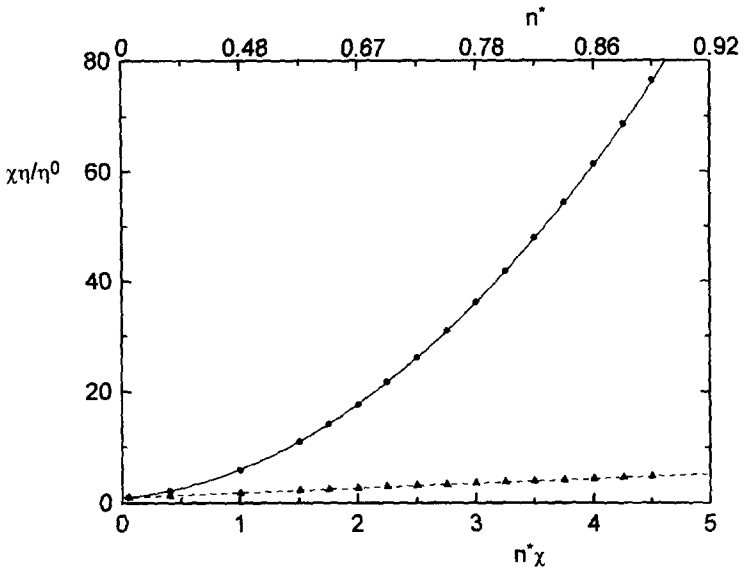

Fig. 1. Plot of $\chi\eta/\eta^0$ (circles and solid line) and of $\chi\eta^k/\eta^0$ (triangles and dashed line) as functions of $n^*\chi$. The symbols are the simulation results and the lines are the theoretical predictions. The top scale corresponds to the reduced density n^*, according to the Carnahan–Starling equation of state, Eq. (10).

larger than $n^* \approx 0.6$ [3], we have considered those densities to check that the ESMC method reproduces the RET even in the high-density domain. As a consistency test [7], we have checked that Eq. (7) is verified by the simulations at all densities. As time evolves, the reduced shear rate a^* decreases, so that the limit in Eqs. (12)–(16) is equivalent to the limit of infinitely long times. In practice, however, one needs to consider finite values of a^* to keep the signal-to-noise ratio within tolerable bounds. Thus, we have evaluated Ψ_1, for instance, by averaging the simulation values of $(P_{yy} - P_{xx})/nk_BTa^{*2}$ over typically the interval $0.04 < a^* < 0.06$.

Fig. 1 shows the simulation values of $\chi\eta/\eta^0$ (circles) and $\chi\eta^k/\eta^0$ (triangles) as functions of the density parameter $n^*\chi$. The error bars are smaller than the size of the symbols and are not drawn. The exact Enskog results, Eqs. (4)–(6), are also plotted. We observe an excellent agreement. Nonlinear effects beyond the Navier–Stokes order are characterized by the viscometric coefficients Ψ_1 and Ψ_2, along with their kinetic parts, and by the excess pressure coefficient γ. They are plotted in Figs. 2–4. The theoretical curves represent now the results recently derived from the RET [12], which were unknown to us at the time when the simulation data were obtained. We can observe a very good agreement in all the cases. In particular, the simulation results are consistent with the theoretical predictions $\Psi_1(n^*\chi) = \Psi_1^{k^2}(n^*\chi)/\Psi_1(0)$, $\gamma(n^*\chi)/(n^*\chi)^2 =$ linear function, and with a change of sign of Ψ_2 and Ψ_2^k at $n^*\chi \simeq 0.36$ ($n^* \simeq 0.25$) and $n^*\chi \simeq 0.60$ ($n^* \simeq 0.36$), respectively.

Finally, we have also estimated the value of the super-Burnett coefficient η_2 defined in Eq. (16) for some characteristic densities. To the best of our knowledge, this

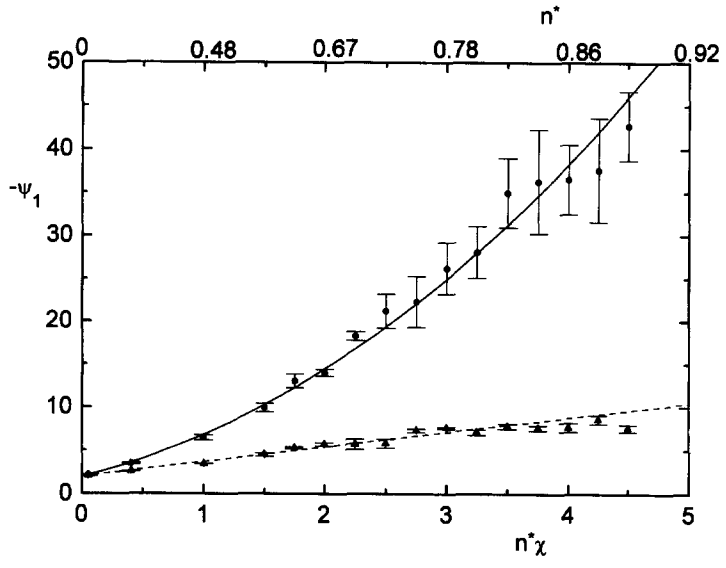

Fig. 2. The same as in Fig. 1, but for $-\Psi_1$ and $-\Psi_1^k$.

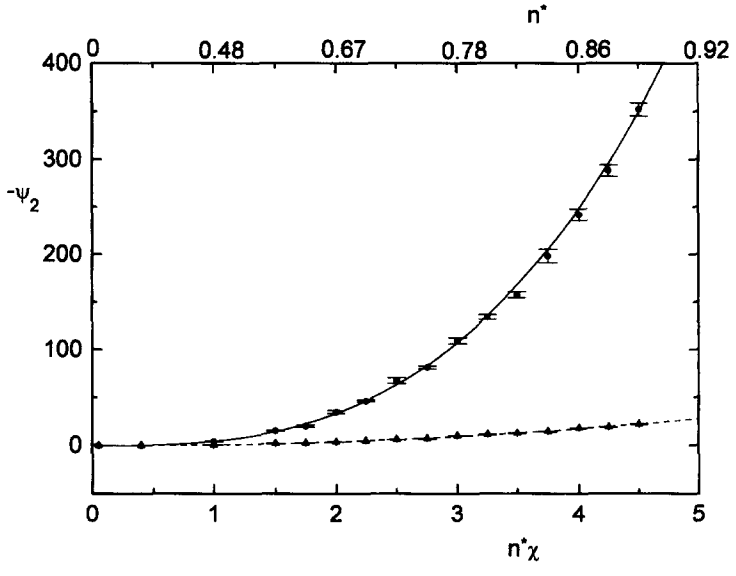

Fig. 3. The same as in Fig. 1, but for $-\Psi_2$ and $-\Psi_2^k$.

coefficient has not been obtained from the RET before. As said in Section 2, a kinetic model recently proposed [8] predicts a change from negative values at low and intermediate densities to positive values at high densities. This means that the non-Newtonian shear viscosity changes from a decreasing function of the shear rate (shear thinning) to an increasing function (shear thickening). Our simulation data confirm this unexpected

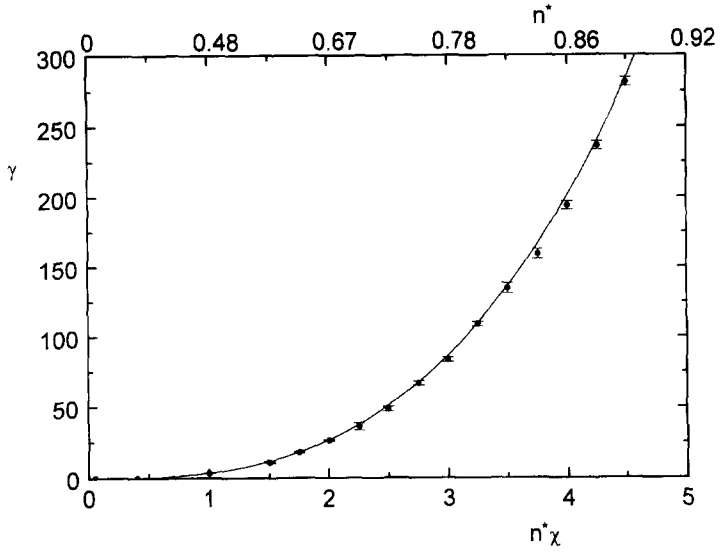

Fig. 4. The same as in Fig. 1, but for γ.

prediction. For instance, we have estimated $\eta_2 \sim -1$ at $n^*\chi = 0.05$ and $\eta_2 \sim +10^3$ at $n^*\chi = 4.5$, with a change of sign at $n^*\chi \approx 2$.

In summary, we have shown that the ESMC algorithm succeeds in capturing the density dependence predicted by the RET for the Navier–Stokes shear viscosity and non-Newtonian transport coefficients. In the particular case of the USF, the computer efficiency of the algorithm is independent of the density and is then the same as that of the DSMC method for the BE. As extra bonuses, our simulation results validate Lutsko's perturbative solution by a moment method [12], as well as the qualitative correctness of the kinetic model proposed in Ref. [8]. The algorithm described in Section 3 is easily extended to include a thermostat force. We plan to undertake simulations with a thermostat far from equilibrium to obtain the shear-rate dependence of the transport coefficients and to analyze the stability of the USF.

Acknowledgements

The authors are grateful to J.F. Lutsko for providing results prior to publication. Partial support from the DGICYT (Spain) through Grant PB94-1021 and from the Junta de Extremadura-Fondo Social Europeo through Grant EIA94-39 is acknowledged.

References

[1] S. Chapman, T.G. Cowling, The Mathematical Theory of Non-Uniform Gases, Cambridge University Press, Cambridge, 1970.

[2] J.H. Ferziger, H.G. Kaper, Mathematical Theory of Transport Processes in Gases, North-Holland, Amsterdam, 1972.

[3] J.R. Dorfman, H. van Beijeren, in: B.J. Berne (Ed.), Statistical Mechanics. Part B: Time-Dependent Processes, Plenum Press, New York, 1977, pp. 65–179.
[4] D. Enskog, Kinetische Theorie der Wärmeleitung, Reibung und Selbstdiffusion in gewissen verdichteten Gasen und Flüssigkeiten, Kungl. Sv. Vetenskapsakademiens Handl. 63 (1922) 3. English transl. in: S.G. Brush (Ed.), Kinetic Theory, vol. 3, Pergamon, New York, 1972, pp. 226–259.
[5] H. van Beijeren, M.H. Ernst, Physica 68 (1973) 437.
[6] T.R. Kirkpatrick, S.P. Das, M.H. Ernst, J. Piasecki, J. Chem. Phys. 92 (1990) 3768.
[7] J.M. Montanero, A. Santos, Phys. Rev. E 54 (1996) 438.
[8] J.W. Dufty, A. Santos, J.J. Brey, Phys. Rev. Lett. 77 (1996) 1270.
[9] G.A. Bird, Molecular Gas Dynamics and the Direct Simulation of Gas Flows. Clarendon Press, Oxford, 1994.
[10] K. Nanbu, in: V. Boffi, C. Cercignani (Eds.), Rarefied Gas Dynamics 15, Teubner, Stuttgart, 1986, pp. 369–383.
[11] F.J. Alexander, A.L. Garcia, B.J. Alder, Phys. Rev. Lett 74 (1995) 5212; in: J.J. Brey, J. Marro, J.M. Rubí, M. San Miguel (Eds.), 25 Years of Non-Equilibrium Statistical Mechanics, Springer, Berlin, 1995, pp. 82–90.
[12] J.F. Lutsko, unpublished.
[13] J.W. Dufty, J.J. Brey, A. Santos, in: G. Ciccotti, W.G. Hoover (Eds.), Molecular-dynamics simulation of statistical-mechanical systems, North-Holland, Amsterdam, 1986, pp. 294–303.
[14] D.J. Evans, G.P. Morriss, Statistical Mechanics of Nonequilibrium Liquids, Academic Press, London, 1990.
[15] N.F. Carnahan, K.E. Starling, J. Chem. Phys. 51 (1969) 635.
[16] D.J. Evans, J. Stat. Phys 57 (1989) 745.